Catalysis Science & Technology

Accepted Manuscript

ROYAL SOCIETY OF CHEMISTRY

www.rsc.org/catalysis

Catalysis Science & Technology

Cite this: DOI: 10.1039/c0xx00000x

www.rsc.org/xxxxxx

PAPER

Superior catalytic performance of $Ce_{1-x}Bi_xO_{2-\delta}$ solid solution and Au/$Ce_{1-x}Bi_xO_{2-\delta}$ for 5-hydroxymethylfurfural conversion in alkaline aqueous solution

Zhenzhen Miao,[a,b] Yibo Zhang,*[a,c] Xiqiang Pan,[d] Tianxiao Wu,[a] Bin Zhang,[a] Jingwei Li,[a,b] Ting Yi,[a,b] Zhengdong Zhang,[a] and Xiangguang Yang*[a,c]

Received (in XXX, XXX) Xth XXXXXXXXX 20XX, Accepted Xth XXXXXXXXX 20XX
DOI: 10.1039/b000000x

Porous Bi-doped ceria ($Ce_{1-x}Bi_xO_{2-\delta}$ solid solution) was prepared by the easy citrate method, and then used as supporting material for Au nanoparticles (NPs) obtained by deposition-precipitation method. In the presence of O_2, $Ce_{1-x}Bi_xO_{2-\delta}$ ($0.08 \le x \le 0.5$) efficiently catalyzed the conversion of 5-hydroxymethylfurfural (HMF) to 5-hydroxymethyl-2-furancarboxylic acid (HFCA) and 2,5-bishydroxymethylfuran (BHMF) in alkaline aqueous solution, without degradation of HMF. The excellent catalytic activity was attributed to the oxygen activation and hydride transfer enhanced by Bi doping and the large amount of oxygen vacancies. After Au NPs supported on $Ce_{1-x}Bi_xO_{2-\delta}$ ($x \le 0.2$), the presence of $Au^{\delta+}$ facilitated the activation of the C-H bond in hydroxymethyl group and then the production of 2,5-furandicarboxylic acid (FDCA) as end-product, inhibiting the generation of BHMF.

Introduction

With the continuous consumption of fossil resources such as oil and natural gas, it is of great importance to exploit and utilize renewable, abundant biomass resources for preparation of bulk and fine chemicals.[1-3] 5-hydroxymethylfurfural (HMF), which can be obtained from dehydration of glucose or fructose,[4, 5] is a compelling platform chemical for the production of 2,5-diformylfuran (DFF), 2,5-bishydroxymethylfuran (BHMF), 5-hydroxymethyl-2-furancarboxylic acid (HFCA) and 2,5-furandicarboxylic acid (FDCA). DFF and BHMF have been regarded as promising monomers for preparing resins, polymers and fine chemicals.[6, 7] HFCA serves not only as a monomer in various polyesters,[8] but also as a starting material for synthesis of FDCA. The presence of two carboxylic groups in FDCA makes it a potential polymer building block which could substitute petro-based terephthalic, isophthalic, and adipic acids.[9]

Many efforts have been made over the past two decades in converting HMF to those more valuable derivatives.[10-14] Vinke et al. firstly reported the oxidation of aqueous HMF into FDCA in near-quantitative yield under basic reaction conditions with a Pt/Al_2O_3 catalyst at 60 °C.[10] Verdeguer et al. demonstrated that high pH was needed to produce FDCA over PtPb/C catalysts and hydroxide base was more effective than carbonate base, which was applicable to the production of HFCA.[11] Davis et al. have shown that the activity of Au catalysts for HMF oxidation was an order of magnitude higher than either Pt or Pd catalysts, but the selectivity to FDCA was much lower than that over the Pt and Pd catalysts.[12]

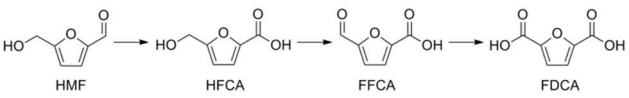

Scheme 1 Oxidation of HMF to FDCA.

The oxidation of HMF comprises of an aldehyde oxidation and an alcohol oxidation (Scheme 1).[15-18] Davis et al.[17] recently elucidated the reaction mechanism that water, rather than O_2, was the source of oxygen atoms inserted into the products by using isotopically-labeled $^{18}O_2$ and $H_2{}^{18}O$. The aldehyde side chain of HMF firstly underwent rapid reversible hydration to a geminal diol intermediate in alkaline aqueous solution. Then, the dehydrogenation of the geminal diol was facilitated by the noble metal catalyst and hydroxide ions. This process produced HFCA and deposited two electrons on the catalyst. The following oxidation of the alcohol group to form 5-formyl-2-furancarboxylic acid (FFCA) was the rate limiting step, as the activation of the C-H bond in the hydroxymethyl group strongly depended on the abilities of catalyst, such as transferring hydride, depositing two additional electrons and interacting with O_2. O_2 was essential for these oxidation processes and played an indirect role via removing the electrons deposited on the catalyst and being reduced to peroxide and hydroxide ions. The aldehyde group of FFCA underwent the same oxidation process in the conversion of HMF to HFCA. Finally, FDCA was obtained.

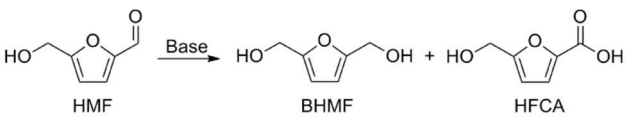

Scheme 2 Cannizzaro reaction of HMF

Notably, although alkaline conditions are favorable for the oxidation of HMF, other competitive reactions could occur at the same time, such as degradation and Cannizzaro reaction of HMF. The Cannizzaro reaction is base-induced disproportionation reaction of an aldehyde lacking a hydrogen atom at an α-position to the carbonyl group. In alkaline medium, one molecule of the aldehyde hydrates to a geminal diol and acts as a hydride donor while the other functions as an acceptor, resulting in a carboxylic acid salt and an alcohol product, respectively. The hydride transfer was the principal component of this redox process.[19] The conversion of HMF to HFCA and BHMF simultaneously via Cannizzaro reaction is of great value (Scheme 2), circumventing using oxidant (for HFCA) or reductor (for BHMF). Recently, Subbiah et al..[13] have investigated the reaction in NaOH aqueous solution. High yields of HFCA and BHMF were obtained when the reactions were conducted at 0 °C for 1 h and then room temperature for certain hours. However, these processes needed a quite long reaction time, such as 18 h, without the presence of catalyst. In addition, the yields were very low at 60 °C even reacted for 24 h, which was due to serious degradation of HMF under basic conditions at higher temperature.

Nanoparticulate CeO_2 with a high external-to-internal atom ratio has a large number of surface oxygen vacancies and defects, which could disperse and stabilize gold nanoparticles (NPs).[20-24] To reach nearly 99% yield of FDCA, the reaction time for Au NPs on nanoparticulate CeO_2 was half for the Au on non-nanometric CeO_2.[15] Reductive pretreatment of the Au/CeO_2 was shown to efficiently increase the catalytic activity, because it increased the amount of Ce^{3+} and oxygen vacancies. The increased Ce^{3+} and oxygen vacancies have shown great importance in transferring hydride and activating O_2 during catalytic oxidation of alcohols in former reports[25]. Corma et al.[25] proposed that Ce^{3+} centers (Lewis acid sites and stoichiometric oxidation sites of CeO_2) and Au^+ species of Au/CeO_2 could readily accept a hydride from C-H bond in alcohol or in the corresponding alkoxide to form Ce-H and Au-H, with the formation of carbonyl compound at the same time. The oxygen vacancies of ceria could activate O_2 and form cerium-coordinated superoxide (Ce-OO•) species which subsequently evolved into cerium hydroperoxide by hydrogen abstraction from Au-H. The cerium hydroperoxide then interacted with Ce-H, producing H_2O and recovering to Ce^{3+} centers. Au-H donated H and changed back to the initial Au^+ species. Without Au^+, the catalytic cycle could not complete.

As discussed above, for ceria base catalyst, increasing the amount of oxygen vacancies would improve the catalytic activity towards HMF conversion. It is favorable for O_2 activation and hydride transfer from HMF (or the geminal diol intermediate) to catalyst. The doping with low-value metal cations to substitute Ce^{IV} in the CeO_2 lattice would drive the formation of a stable O-deficient bulk fluorite-type structure to maintain charge conservation. Ce^{3+} centers would increase with the creation of oxygen vacancies.[26] Cubic δ-Bi_2O_3 has an atomic configuration of C-type rare earth sesquioxide, which is similar to CeO_2. As an oxide ionic conductor, it could release oxygen at low temperature, leading that the Bi-doped CeO_2 has a higher low-temperature redox activity towards CeO_2.[27, 28] Glaeser et al.[29] have also indicated that the lone pair electrons of Bi^{3+} was the active site for O_2 activation, and oxide ion of Bi-O-M could help the hydrogen transfer from reaction substrate to the catalyst in selective oxidation. Thus, the Bi-doped CeO_2 may serve as admirable catalyst for Cannizzaro reaction of HMF or excellent support of Au NPs for HMF oxidation.

Herein, a series of $Ce_{1-x}Bi_xO_{2-\delta}$ ($x \leq 0.5$) were synthesized by the easy citrate method and used as supports for gold NPs obtained via a deposition-precipitation method. $Ce_{1-x}Bi_xO_{2-\delta}$ and $Au/Ce_{1-x}Bi_xO_{2-\delta}$ were all examined in HMF conversion in alkaline aqueous solution. Interestingly, in the presence of O_2, $Ce_{1-x}Bi_xO_{2-\delta}$ ($0.08 \leq x \leq 0.5$) could catalyze HMF transform into HFCA and BHMF at 65 °C without degradation of HMF. $Au/Ce_{1-x}Bi_xO_{2-\delta}$ ($0.08 \leq x \leq 0.2$) catalysts showed significantly improved catalytic activities towards HMF oxidation to FDCA compared to Au/CeO_2. To the best of our knowledge, it is the first report about the Cannizzaro reaction of HMF catalyzed by non-precious metal oxide in eco-friendly aqueous solution.

Experimental

Chemicals and Characterization

All the reagents were used as received without further purification. HMF (98%), HFCA, 5-Formyl-2-furancarboxylic Acid (FFCA, 98%), FDCA (97%) were obtained from J & K Co. Ltd (Beijing, China). $Ce(NO_3)_3 \cdot 6H_2O$, $Bi(NO_3)_3 \cdot 5H_2O$ were purchased from Aladdin Chemicals Co. Ltd (Shanghai, China). Concentrated HNO_3, concentrated H_2SO_4, KOH, citric acid monohydrate were purchased from Beijing Chemicals Co. Ltd (Beijing, China). $HAuCl_4 \cdot 4H_2O$ was obtained from Shanghai Chemical reagent Co. Ltd (Shanghai, China).

The powder X-ray diffraction (XRD) patterns were carried out on a Bruker D8 Advance X-ray diffractometer using a Cu Kα radiation source (λ = 1.5406 Å). Scanning electron microscopy (SEM) was performed on a field emission Hitachi S-4800 instrument. Transmission electron microscopy (TEM) was performed using a FEI Tecnai G2 S-Twin instrument with a field emission gun operating at 200 kV. Raman spectra were collected through a Renishaw 2000 model confocal microscopy Raman spectrometer with a CCD detector and a holographic notch filter (Renishaw Ltd., Gloucestershire, U.K.) at ambient conditions, using the radiation of 514.5 nm. H_2-TPR experiment was conducted on a self-made chemisorption instrument equipped with a thermal conductivity detector (TCD).[30] 50 mg of fresh samples were loaded into a quartz reactor at room temperature and reduced in a flowing 5% H_2/Ar mixed gas with a heating rate of 10 °C /min. The effluent gas was analyzed with the TCD. The nitrogen adsorption-desorption isotherms of the samples were measured with a Autosorb-iQ-Station-1 instrument at 77 K after pretreated at 473 K for 10 h under high vacuum. The specific surface areas were determined by Brunauer-Emmett-Teller (BET) equation. Elemental contents were measured by ICP-OES (iCAP 6300 Thermo Scientific USA). X-ray photoelectron spectroscopy (XPS) spectra were obtained on a VG Thermo ESCALAB 250 spectrometer operated at 120 W. All the binding energies were calibrated using the $Ce^{4+}(3d^{10}4f^0V^n)$ ($u^{///}$) signal at 916.6 eV to remove surface charging effects.[31] Liquid state ^1H NMR spectra were recorded at 298 K on a Bruker Avance 300 NMR spectrometer.

Catalyst preparation

A series of $Ce_{1-x}Bi_xO_{2-\delta}$ mixed oxides with x = 0, 0.05, 0.08, 0.1, 0.125, 0.15, 0.2, 0.5 were prepared by the citrate acid method.[32] In a typical synthesis, stoichiometric amounts of $Bi(NO_3)_3{\cdot}5H_2O$ and $Ce(NO_3)_3{\cdot}6H_2O$ (Bi + Ce = 0.1 mol) were mixed in an appropriate concentration of nitric acid solution to obtain a clear solution. Citric acid monohydrate was then added to the mixture (metal cation to ligand molar ratio was 1:2). The as-prepared solution was heated on a hot plate at 200 °C under stirring. Continuous heating process turned this solution to white (without Bi) or yellow gel, which was afterwards combusted with flame and yielded highly spongy and uneven color bulk particles. Finally, the precursors were calcined at 500 °C for 2 h to obtain $Ce_{1-x}Bi_xO_{2-\delta}$ mixed oxides. The color of Bi-doped ceria samples was yellow and deepened with increasing the amount of Bi doping (Fig. S1).

Gold NPs were deposited on $Ce_{1-x}Bi_xO_{2-\delta}$ via a deposition-precipitation method.[33] 15 ml of 8 mM $HAuCl_4$ aqueous solution was sampled into a round bottom flask, 1.0 M KOH was then added dropwise to the stirred solution until the pH value was adjusted to 10. The resulting solution was heated at 80 °C in an oil bath. 2.0 g $Ce_{1-x}Bi_xO_{2-\delta}$ was added and the pH value was readjusted to 10. The suspension kept stirring for another 2 h, then centrifuged and washed four times with water, dried at 40 °C for 2 days. The $Au/Ce_{1-x}Bi_xO_{2-\delta}$ samples were calcined at 200 °C for 2.5 h before use.

HMF conversion in alkaline aqueous solution

The aqueous phase catalytic conversion of HMF was carried out in a 50 ml autoclave with PTFE liner and equipped with a magnetic stirrer. In a typical experiment, 6 ml of the reactant solution (0.15 M HMF and 0.6 M NaOH) was added to the reactor along with the appropriate amount of catalyst. The reactor was purged for 3 times with O_2 and then pressurized at 1.0 MPa. Timing was started once the reactor was placed in a preheated oil bath pot under stirring. After reacting a certain time, the samples were centrifuged, diluted with deionized H_2O for 50 times and acidified with sulfuric acid. The resulted solutions were filtered by using a syringe filter (0.2 μm) before analysis in a high performance liquid chromatograph (HPLC) equipped with a Waters 2487 Dual λ absorbance detector. The HPLC utilized a Bio-Rad Aminex HPX-87H column at 35 °C and 5 mM H_2SO_4 flowing at 0.5 ml·min^{-1} to perform the separation. Identification and calibration of FDCA, HFCA, FFCA and HMF were determined by injecting known concentrations.

Results and discussion

Table 1 Textural properties of the typical $Ce_{1-x}Bi_xO_{2-\delta}$ samples

Sample	Surface area (m^2/g)	Pore diameter (nm)[a]	Average pore volume (cm^3/g)[b]
CeO_2	117.90	3.83	0.35
$Ce_{0.95}Bi_{0.05}O_{2-\delta}$	93.72	3.81	0.32
$Ce_{0.9}Bi_{0.1}O_{2-\delta}$	81.11	3.82	0.29
$Ce_{0.8}Bi_{0.2}O_{2-\delta}$	46.25	3.82	0.24
$Ce_{0.5}Bi_{0.5}O_{2-\delta}$	24.34	3.82	0.15

[a] Calculated by BJH method from desorption branch. [b] Estimated by single point adsorption at relative pressure of 0.99.

The as-prepared samples were proved to be porous material. SEM images shown in Fig. S2 illustrated the presence of macropores larger than 50 nm. The nitrogen physisorption analysis results of the $Ce_{1-x}Bi_xO_{2-\delta}$ (x = 0, 0.05, 0.1, 0.2, 0.5) samples are summarized in Table 1. The adsorption isotherms and pore size distribution curves are presented in Fig. S3. The adsorption-desorption isotherms of all the samples showed type IV isotherm with a hysteresis loop, indicating that these samples were mainly in the mesoporous range of 2-50 nm. The pore size was centered at about 3.8 nm. In addition, the specific surface area of CeO_2 was calculated to be 117.90 m^2/g and the total pore volume was 0.35 cm^3/g which both decreased with increasing the amount of Bi doping.

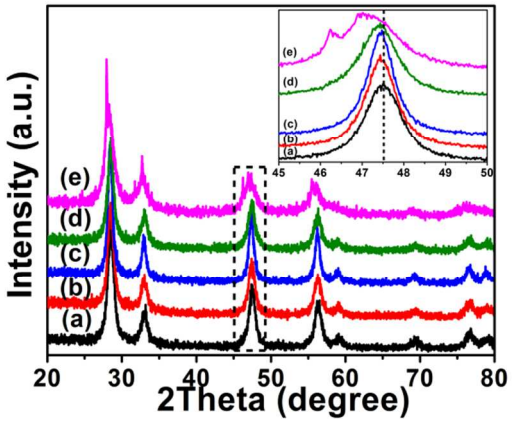

Fig. 1 XRD patterns of (a) CeO_2, (b) $Ce_{0.95}Bi_{0.05}O_{2-\delta}$, (c) $Ce_{0.9}Bi_{0.1}O_{2-\delta}$, (d) $Ce_{0.8}Bi_{0.2}O_{2-\delta}$ and (e) $Ce_{0.5}Bi_{0.5}O_{2-\delta}$ (inset: XRD of samples scanned at low speed).

The powder XRD patterns of $Ce_{1-x}Bi_xO_{2-\delta}$ ($x \leq 0.2$) samples showed in Fig. 1 demonstrate that only peaks attributed to a cubic fluorite structure of CeO_2 (JCPDS 34-0394) were observed and no other phase was detected. Compared with the pure CeO_2 sample, the diffraction peaks of the Bi-doped samples were slightly shifted to lower angle (inset of Fig. 1), indicating the expansion of the unit cell of CeO_2. This variation could be intelligibly ascribed to Ce^{4+} with ionic radius of 0.97 Å partially replaced by Bi^{3+} (1.17 Å) and the formation of solid solution. For $Ce_{0.5}Bi_{0.5}O_{2-\delta}$ sample, in addition to the low value-shifted peaks of CeO_2, peaks located at around 28.0° and 46.2° appeared, which could be ascribed to Bi_2O_3 (JCPDS 65-1209).

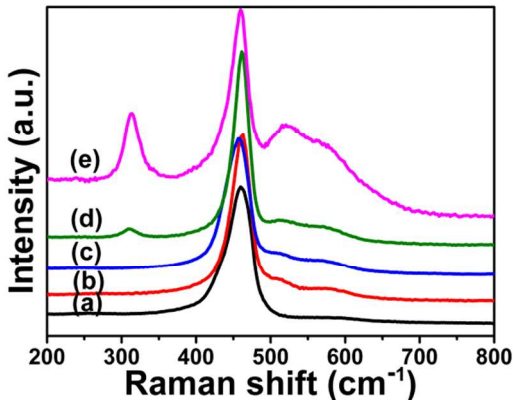

Fig. 2 Raman spectra of (a) CeO_2, (b) $Ce_{0.95}Bi_{0.05}O_{2-\delta}$, (c) $Ce_{0.9}Bi_{0.1}O_{2-\delta}$, (d) $Ce_{0.8}Bi_{0.2}O_{2-\delta}$ and (e) $Ce_{0.5}Bi_{0.5}O_{2-\delta}$.

Raman spectra of $Ce_{1-x}Bi_xO_{2-\delta}$ (x = 0, 0.05, 0.1, 0.2, 0.5) samples are presented in Fig. 2. The main peak at ca. 460 cm^{-1} was assigned to the F_{2g} mode vibration of CeO_2 cubic fluorite structure.[34] The Bi doped samples also showed two peaks at ca. 520 and 580 cm^{-1}, which could be indexed to the presence of Bi^{3+} ions[35] and oxygen vacancies generated as charge compensating defects[36], respectively. For CeO_2, a very weak peak at ca. 580 cm^{-1} was also observed, suggesting the presence of a small number of oxygen vacancies in CeO_2 possibly caused in the violent and rough citrate-method process. It was obvious that the oxygen vacancies peak enhanced significantly after Bi doping, implying the increase of the amount of oxygen vacancies. When the relative content of Bi reached to 20 mol%, a characteristic peak of Bi_2O_3 at ca. 325 cm^{-1} appeared.[37, 38] The Bi_2O_3 phase could not be detected by XRD analysis, suggesting that Bi_2O_3 species should be at a low content and disperse well in $Ce_{0.8}Bi_{0.2}O_{2-\delta}$.

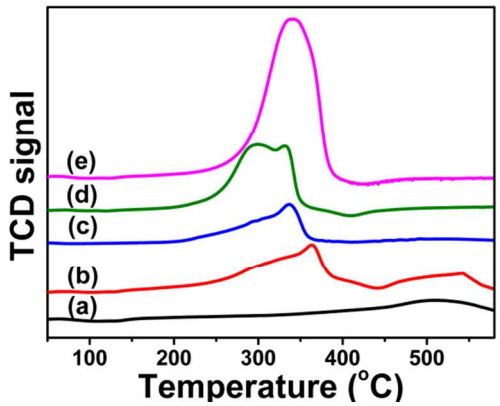

Fig. 3 H_2-TPR profiles of (a) CeO_2, (b) $Ce_{0.95}Bi_{0.05}O_{2-\delta}$, (c) $Ce_{0.9}Bi_{0.1}O_{2-\delta}$, (d) $Ce_{0.8}Bi_{0.2}O_{2-\delta}$ and (e) $Ce_{0.5}Bi_{0.5}O_{2-\delta}$.

In order to figure out the low-temperature redox activity of $Ce_{1-x}Bi_xO_{2-\delta}$, the reduction profiles of the samples were taken and the results are shown in Fig. 3. The H_2 reduction maximum of Bi-doped samples occurred at 200-400 °C associated with the reduction of Ce^{4+} and Bi^{3+}. The temperature was much lower than that of pure ceria, indicating the more reducible property of the Bi-doped samples. Higher oxygen release capacity of the Bi-doped samples could also be found, as the peak area increased with the amount of Bi doping. The results also indicated that the amount of the stoichiometric oxidation sites showed the similar behavior.

Table 2 HMF reaction in alkaline aqueous solution over $Ce_{1-x}Bi_xO_{2-\delta}$ catalysts[a]

Entry	Catalyst	HMF Conversion[b] (%)	Y_{FDCA}[b] (%)	Y_{HFCA}[b] (%)	Y_{BHMF}[d] (%)
1	-	93	-	4	-
2	CeO_2	97 (100)[c]	- (9)[c]	15 (19)[c]	9
3	$Ce_{0.95}Bi_{0.05}O_{2-\delta}$	99	2	26	21
4	$Ce_{0.92}Bi_{0.08}O_{2-\delta}$	99	5	48	46
5	$Ce_{0.9}Bi_{0.1}O_{2-\delta}$	100	5	53	42
6	$Ce_{0.875}Bi_{0.125}O_{2-\delta}$	100 (100)[c]	2 (90)[c]	64 (10)[c]	33
7	$Ce_{0.85}Bi_{0.15}O_{2-\delta}$	100	2	65	32
8	$Ce_{0.8}Bi_{0.2}O_{2-\delta}$	100	3	60	36
9	$Ce_{0.5}Bi_{0.5}O_{2-\delta}$	100	8	58	33

[a] General conditions: 0.15 M HMF solution in 0.6 M NaOH (6 ml), 0.1 g catalyst, 65 °C, 1.0 MPa O_2. [b] Conversion or product yield determined by HPLC after reacted for 1 h. [c] Yield after the reaction supernatant reacted for another 1 h at the same conditions by using $Au/Ce_{0.9}Bi_{0.1}O_{2-\delta}$ (Au : HMF = 6.67×10^{-3} mol/mol) catalyst. [d] Yield determined by GC-MS after reacted for 1 h.

HMF conversion in alkaline aqueous solution was carried out with or without $Ce_{1-x}Bi_xO_{2-\delta}$ samples. The conversion of HMF and the yields of FDCA and HFCA that determined by HPLC analysis are listed in Table 2. As we knew, HMF was prone to degrade in alkaline aqueous solution, especially at high temperature. The red-brown solution obtained with the formation of by-products such as levulinic and formic acids.[18] When $Ce_{1-x}Bi_xO_{2-\delta}$ (x = 0, 0.05) or no catalyst was added into the reaction system, the resulted reaction solutions after 1 h at 65 °C were red-brown with low yields of HFCA (Table 2, entries 1-3). However, with $Ce_{1-x}Bi_xO_{2-\delta}$ ($0.08\leq x\leq0.5$) in the reaction system, the resultant solutions were nearly colorless and the yields of HFCA were high (Table 2, entries 4-9). The results may be ascribed to the presence of abundant stoichiometric oxidation sites in $Ce_{1-x}Bi_xO_{2-\delta}$ ($0.08\leq x\leq0.5$).

To further explain the results, following experiments were performed. After reacted over CeO_2 or $Ce_{0.875}Bi_{0.125}O_{2-\delta}$ for 1h, the reaction solution was centrifuged. The obtained supernatant was reacted for another hour by using $Au/Ce_{0.9}Bi_{0.1}O_{2-\delta}$ catalyst at the same conditions. Interestingly, the $Ce_{0.875}Bi_{0.125}O_{2-\delta}$ system obtained 90% yield of FDCA and 10% yield of HFCA (Table 2, entry 6) while CeO_2 just did a total 28% yield of FDCA and HFCA (Table 2, entry 2). Obviously, there was no degradation of HMF occurred with the presence of $Ce_{0.875}Bi_{0.125}O_{2-\delta}$ in alkaline aqueous solution. The product undetected by HPLC analysis after 1 h over $Ce_{0.875}Bi_{0.125}O_{2-\delta}$ was ought to BHMF. BHMF was the Cannizzaro reaction product[13, 17] and did not respond to UV[39] (Table 2, entry 6). ^1H NMR analysis also proved it (Fig. S4). Then, the BHMF yields of these reactions were determined by gas chromatography-mass spectrometry (GC-MS) analysis after extracting the resulted reaction solutions by ethyl ether (Fig. S5). The results are also listed in Table 2.

Table 3 HMF reaction at different atmosphere over $Ce_{0.875}Bi_{0.125}O_{2-\delta}$[a]

Entry	atmosphere	HMF Conversion[b] (%)	Y_{FDCA}[b] (%)	Y_{HFCA}[b] (%)
1	1.0 MPa O_2	100	2	64
2[c]	air	97	1	24
3	1.0 MPa Ar	98	1	16

[a] General conditions: 0.15 M HMF solution in 0.6 M NaOH (6 ml), 0.1 g $Ce_{0.875}Bi_{0.125}O_{2-\delta}$, 65 °C. [b] Conversion or product yield determined by HPLC after reacted for 1 h. [c] Reaction autoclave was sealed after all the reactants were added without purging with any gas.

Under air or 1.0 MPa Ar atmosphere and otherwise the same conditions, reactions with $Ce_{0.875}Bi_{0.125}O_{2-\delta}$ all resulted in sepia solutions and low yields of HFCA (Table 3, entries 2, 3). These results indicated that O_2 was essential for HMF conversion catalyzed by $Ce_{0.875}Bi_{0.125}O_{2-\delta}$ and there was strong interaction between $Ce_{1-x}Bi_xO_{2-\delta}$ ($0.08\leq x\leq 0.5$) and O_2. Other M-doped $Ce_{0.9}M_{0.1}O_{2-\delta}$ (M = Y, La, Mn, Fe) samples were also examined in HMF conversion in the presence of O_2 (1.0 MPa). They all resulted in serious degradation of HMF with low yields of HFCA (Table. S1). It implied that the Bi-doped CeO_2 was unique for O_2 activation during HMF conversion in alkaline aqueous solution.

16% yield of HFCA was obtained under 1.0 MPa Ar atmosphere (Table 3, entry 3). It meant that $Ce_{0.875}Bi_{0.125}O_{2-\delta}$ contained large amount of stoichiometric oxidation sites and acted as oxygen donor.[40-42] When gaseous oxygen was introduced into the reaction system, $Ce_{0.875}Bi_{0.125}O_{2-\delta}$ could act as an oxygen pump, releasing and adsorbing oxygen through a redox process. The redox process involved the variation of the two oxidation states of Ce (III and IV) and related to the exotic highly reductive Bi^{3+}. The lone pair electrons of Bi^{3+} and the large amount of oxygen vacancies facilitated the O_2 adsorption and dissociation during this process.[27-29] As a result, the present O_2 in the reaction system replenished the consumed lattice oxygen (mainly oxide ions of the Bi-O-Ce linkages) in $Ce_{0.875}Bi_{0.125}O_{2-\delta}$ and avoided $Ce_{0.875}Bi_{0.125}O_{2-\delta}$ from deactivating, leading to the transformation of HMF via Cannizzaro reaction without degradation.[43, 44]

Subbiah et al.[13] have shown that Cannizzaro reaction of HMF could be performed at room temperature without catalyst in NaOH aqueous solution. The reaction time was up to 18 h. The 43% yield of BHMF and 44% yield of HFCA that obtained under the optimized reaction conditions suggested more than 10% degradation of HMF. Moreover, serious decomposition of HMF was found at higher temperature (60 °C), producing only 22% total yield of BHMF and HFCA even after 24 h. In our system, however, the degradation of HMF was inhibited even at 65 °C, and the reaction time for 100% conversion of HMF reduced greatly to less than 1 h with the presence of $Ce_{1-x}Bi_xO_{2-\delta}$ ($0.08\leq x\leq 0.5$) and 1.0 MPa O_2 in the reaction system simultaneously (Table 2, entries 4-9). The reaction efficiency was improved greatly.

A 66% total yield of carboxylic acid products (more than 50%) was obtained under 1.0 MPa O_2 pressure over $Ce_{0.875}Bi_{0.125}O_{2-\delta}$ catalyst (Table 2, entry 6). It implied that Cannizzaro reaction and oxidation of HMF proceeded simultaneously. The geminal diol intermediate was firstly formed via rapid reversible hydration of HMF.[17, 40] Then, it partly reacted with the aldehyde moiety of HMF and obtained the Cannizzaro reaction products HFCA and BHMF equivalently,[13, 19] while others underwent the oxidation of geminal diol or hydroxymethyl group and yielded HFCA or FDCA. The electrons generated during the oxidation reaction were removed by molecular oxygen, and the catalytic cycle closed.[17] The oxidation and Cannizzaro reaction both involved hydride transfer from geminal diol and the Bi-doped CeO_2 showed unique performance towards the reaction system. Therefore, we summarized that the presence of Bi-O-Ce linkages and Ce^{3+} centers, together with the lone pair electrons of Bi^{3+} and large amount of oxygen vacancies, assisted $Ce_{0.875}Bi_{0.125}O_{2-\delta}$ transferring hydride and activating O_2, thereby catalysing the reaction.[25, 29]

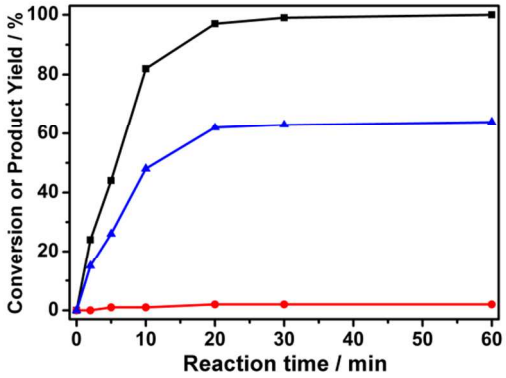

Fig. 4 HMF conversion and product yields as a function of reaction time during HMF reaction in aqueous solution over $Ce_{0.875}Bi_{0.125}O_{2-\delta}$ catalyst (0.1 g $Ce_{0.875}Bi_{0.125}O_{2-\delta}$, 4 equiv. NaOH, 1.0 MPa O_2, 65 °C; HMF: ■, HFCA: ▲, FDCA: ●).

As shown in Fig. 4, HMF was quickly transformed to products with the presence of O_2 and $Ce_{0.875}Bi_{0.125}O_{2-\delta}$. A 97% conversion of HMF was achieved only after 20 min. It further indicated the excellent properties of $Ce_{0.875}Bi_{0.125}O_{2-\delta}$ towards activating oxygen and transferring hydride. $Ce_{0.875}Bi_{0.125}O_{2-\delta}$ itself showed weak ability to activate the cleavage of C-H bond in hydroxymethyl group, resulted in the low yield of FDCA and large amount of BHMF.

Table 4 Catalytic activity of $Au/Ce_{1-x}Bi_xO_{2-\delta}$ towards HMF oxidation[a]

Entry	Catalyst	Au loading[b] (wt%)	HMF Conversion[c] (%)	Y_{FDCA}[c] (%)	Y_{HFCA}[c] (%)
1	Au/CeO_2	1.02	100	39	57
2	$Au/Ce_{0.95}Bi_{0.05}O_{2-\delta}$	1.04	100	46	49
3	$Au/Ce_{0.92}Bi_{0.08}O_{2-\delta}$	1.05	100	73	27
4	$Au/Ce_{0.9}Bi_{0.1}O_{2-\delta}$	1.11	100	74	26
5	$Au/Ce_{0.875}Bi_{0.125}O_{2-\delta}$	1.07	100	75	25
6	$Au/Ce_{0.85}Bi_{0.15}O_{2-\delta}$	1.09	100	77	23
7	$Au/Ce_{0.8}Bi_{0.2}O_{2-\delta}$	1.10	100	74	26
8	$Au/Ce_{0.5}Bi_{0.5}O_{2-\delta}$	1.10	99	4	56

[a] General conditions: 0.15 M HMF solution in 0.6 M NaOH (6 ml), Au : HMF = 6.67×10^{-3} mol/mol, 65 °C, 1.0 MPa O_2. [b] From ICP analysis. [c] Conversion or product yield determined by HPLC after reacted for 1 h.

All the $Au/Ce_{1-x}Bi_xO_{2-\delta}$ samples showed similar Au loading around 1 wt%. To compare their catalytic activities, they were all applied in the oxidation of HMF at the same reaction conditions for 1 h. The results are listed in Table 4. Besides $Au/Ce_{0.5}Bi_{0.5}O_{2-\delta}$, all the Bi-doped catalysts displayed higher FDCA yield with respect to Au/CeO_2. $Au/Ce_{1-x}Bi_xO_{2-\delta}$ ($0.08\leq x\leq 0.2$) catalysts were active enough to catalyze the oxidation of HMF to HFCA and FDCA (Table 4, entries 3-7). However, $Au/Ce_{1-x}Bi_xO_{2-\delta}$ ($x = 0$, 0.05) catalysts resulted in not only low yields of FDCA but also the production of some degradation products (Table 4, entries 1, 2). The favorable catalytic activity of $Au/Ce_{1-x}Bi_xO_{2-\delta}$ ($0.08\leq x\leq 0.2$) towards HMF oxidation was attributed to the presence of $Au^{\delta+}$ and Bi doping. $Au^{\delta+}$ in the $Au/Ce_{1-x}Bi_xO_{2-\delta}$ catalysts assisted the oxidation of alcohol, including turning alcohol into metal-alkoxide intermediate and activating the C-H bond. Besides, in the whole oxidation process, the hydride transferred from C-H bond could not only combine with Ce^{3+} and

$Au^{\delta+}$, but also with oxygen ions of Bi-O-Ce linkages and Ce^{3+}-O_2 centers.[16, 25, 45] The electrons generated during the hydride transfer were captured by Au clusters and the reducible $Ce_{1-x}Bi_xO_{2-\delta}$ support, and then released when the $Au/Ce_{1-x}Bi_xO_{2-\delta}$ interacted with molecular O_2.[17, 46] As the geminal diol intermediate was more easily oxidized, the Cannizzaro reaction was inhibited over $Au/Ce_{1-x}Bi_xO_{2-\delta}$ ($x\leq0.2$) catalysts. Oxidation products HFCA and FDCA were yielded without the formation of BHMF. Based on the above analysis, the first two reaction processes are listed in Scheme 3.

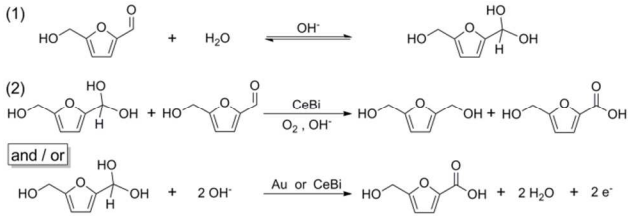

Scheme 3 The first two reaction processes of HMF conversion in alkaline aqueous solution. CeBi represents $Ce_{1-x}Bi_xO_{2-\delta}$ ($0.08\leq x\leq0.5$) and Au represents $Au/Ce_{1-x}Bi_xO_{2-\delta}$ ($x\leq0.2$).

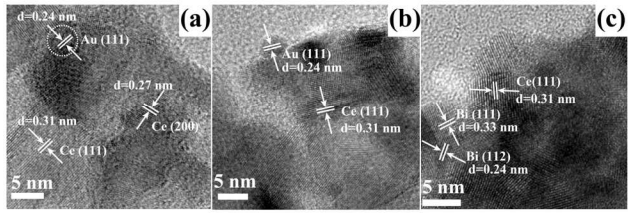

Fig. 5 HRTEM of (a, b) $Au/Ce_{0.9}Bi_{0.1}O_{2-\delta}$ and (c) $Au/Ce_{0.5}Bi_{0.5}O_{2-\delta}$ after reacted for 1 h.

TEM images of $Au/Ce_{1-x}Bi_xO_{2-\delta}$ ($x = 0.1, 0.5$) after reacted for 1 h are shown in Fig. 5. Because of the low loading amount of Au and the low contrast between Au and ceria, Au particles were hardly detectable by TEM.[47] Only a few nanocrystals with a size of about 4 nm were identified as the gold phase on $Au/Ce_{0.9}Bi_{0.1}O_{2-\delta}$ catalyst (Fig. 5a, b), and no Au particle was found on the $Au/Ce_{1-x}Bi_xO_{2-\delta}$ ($x = 0, 0.2, 0.5$) catalysts. XRD patterns of all the samples are shown in Fig. S6. No characteristic diffraction peak corresponding to gold (38.2°, 44.3°) was observed. Bi_2O_3 phase was also found in the $Au/Ce_{0.5}Bi_{0.5}O_{2-\delta}$ sample by TEM (Fig. 5c).

Table 5 XPS Au 4f peak analysis for $Au/Ce_{1-x}Bi_xO_{2-\delta}$ catalysts after reacted for 1 h.

sample	XPS Au 4f peak		
	Au^0	Au^+	Au^{3+}
Au/CeO_2	44.0	34.9	21.1
$Au/Ce_{0.9}Bi_{0.1}O_{2-\delta}$	54.4	45.6	-
$Au/Ce_{0.8}Bi_{0.2}O_{2-\delta}$	62.2	37.8	-
$Au/Ce_{0.5}Bi_{0.5}O_{2-\delta}$	75.4	24.6	-

Quantitative fitting of the Au (4f) peaks of $Au/Ce_{1-x}Bi_xO_{2-\delta}$ ($x = 0, 0.1, 0.2, 0.5$) catalysts after reacted for 1 h are shown in table 5 and Fig. S7. It is well documented in the literature that the electronic state of surface gold NPs depends on the size of gold NPs and the nature of supports, and always plays an important role in the oxidation reaction.[48] For alcohol oxidation catalyzed by Au/CeO_2, $Au^{\delta+}$ was considered as the active site on Au clusters.[23, 25, 46] There existed about 25% of $Au^{\delta+}$ in $Au/Ce_{0.5}Bi_{0.5}O_{2-\delta}$ catalyst, which might be too low to afford the activation of the C-H bond in alcohol, and resulted in the low yield of FDCA (Table 4, entry 8). Here, we also noticed that after calcination at 200 °C for 2.5 h, the $Au/Ce_{1-x}Bi_xO_{2-\delta}$ ($x\leq0.15$) samples turned to purple, while $Au/Ce_{0.8}Bi_{0.2}O_{2-\delta}$ was sap green and $Au/Ce_{0.5}Bi_{0.5}O_{2-\delta}$ was emerald. It implied the presence of different Au species in $Au/Ce_{1-x}Bi_xO_{2-\delta}$ catalysts. In addition, the color of these catalysts deepened after NaOH added into the reaction mixture, which was similar to a previous report.[48]

The above results demonstrated that the $Au/Ce_{1-x}Bi_xO_{2-\delta}$ ($0.08\leq x\leq0.2$) catalysts were preferable for HMF oxidation to FDCA. $Au/Ce_{0.9}Bi_{0.1}O_{2-\delta}$ was selected to further investigate the effect of the reaction parameters, such as amount of base, temperature, oxygen pressure, HMF/Au molar ratio and reaction time. The results are shown in Fig. S8-11.

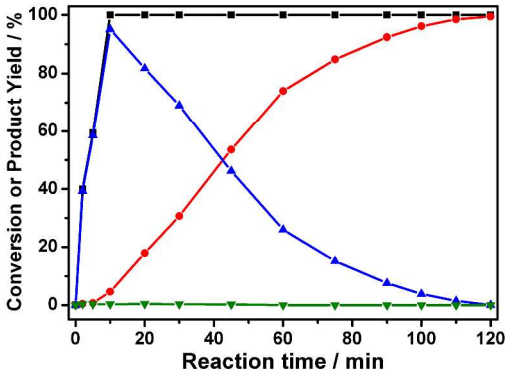

Fig. 6 HMF conversion and product yields as a function of reaction time in the oxidation of HMF in aqueous solution over $Au/Ce_{0.9}Bi_{0.1}O_{2-\delta}$ catalyst (Au : HMF = 6.67×10^{-3} mol/mol, 4 equiv. NaOH, 1.0 MPa O_2, 65 °C; HMF: ■, FDCA: ●, HFCA: ▲, FFCA: ▼).

4 equiv. NaOH, 1.0 MPa O_2, 65 °C and HMF/Au molar ratio 150 were chosen to study the effect of reaction time over $Au/Ce_{0.9}Bi_{0.1}O_{2-\delta}$ catalyst. As shown in Fig. 6, the aldehyde moiety of HMF was quickly oxidized to carboxylic acid at the initial stage of the reaction, 100% conversion of HMF and 95% yield of HFCA were achieved only after 10 min. That stressed the superiority of $Ce_{1-x}Bi_xO_{2-\delta}$ for HMF conversion. Subsequently, the amount of HFCA slowly decreased while the yield of FDCA increased. There only a little FFCA was detected within the first 45 min, indicating that the oxidation of alcohol group to aldehyde was the rate limiting step. It was identical with previous reports.[15]

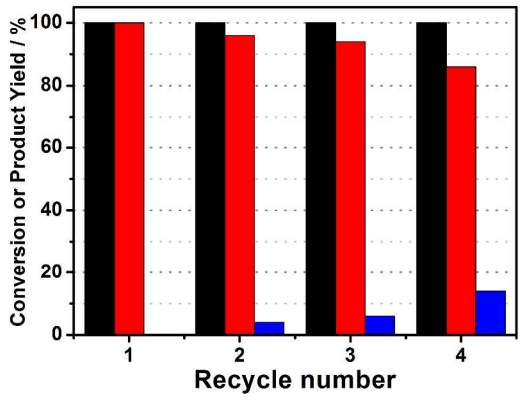

Fig. 7 Reusability study of $Au/Ce_{0.9}Bi_{0.1}O_{2-\delta}$ catalyst in the oxidation of HMF in aqueous solution (Au : HMF = 6.67×10^{-3} mol/mol, 4 equiv. NaOH, 1.0 MPa O_2, 65 °C, 2 h; HMF: black, FDCA: red, HFCA: blue).

Catalyst recycling was also studied for the $Au/Ce_{0.9}Bi_{0.1}O_{2-\delta}$ catalyst. After the catalyst was recovered by filtration, washed with water and dried at 60 °C, a new set of HMF oxidation experiments were carried out (Fig. 7). The presence and quantity of Au element in the filtrate was analyzed by ICP-OES analysis, thus excluding the hypothesis of Au leaching. The catalyst could be used for three times without much loss of activity under identical reaction conditions. The yield of FDCA was only 86% after the fourth use, but the solution after reaction was also colorless and there was almost no other by-product besides HFCA. We could deem that increasing the reaction time would also result a >99% yield of FDCA. After using for three times, we found that large catalyst particles appeared. The decrease of the FDCA selectivity may be due to the agglomeration of the catalyst or the adsorption of organic molecules onto partial active sites of the catalyst.

Conclusions

In this work, a series of porous Bi-doped ceria were prepared by the easy citrate method. XRD and Raman analysis indicated that $Ce_{1-x}Bi_xO_{2-\delta}$ solid solutions were obtained with large amount of oxygen vacancy defects. In the presence of O_2, $Ce_{1-x}Bi_xO_{2-\delta}$ ($0.08\leq x\leq0.5$) efficiently catalyzed HMF into BHMF and HFCA in alkaline aqueous solution. Nearly completely conversion of HMF (97%) was reached only in 20 min at 65 °C and 1.0 MPa O_2, without degradation of HMF. The superior catalytic properties of $Ce_{1-x}Bi_xO_{2-\delta}$ ($0.08\leq x\leq0.5$) were attributed to the specific Bi doping. O_2 activation and hydride transfer were enhanced by the lone pair electrons of Bi^{3+} and the presence of Bi-O-Ce linkages together with large amount of Ce^{3+} centers and oxygen vacancies. The presence of $Au^{\delta+}$ in the $Au/Ce_{1-x}Bi_xO_{2-\delta}$ ($x\leq0.2$) catalysts assisted the oxidation of alcohol, especially the geminal diol intermediate, yielding FDCA as end-product without BHMF. >99% yield of FDCA was obtained after 2 h over $Au/Ce_{0.9}Bi_{0.1}O_{2-\delta}$ catalyst. $Ce_{1-x}Bi_xO_{2-\delta}$ ($0.08\leq x\leq0.5$) may be also applicable for other Cannizzaro reactions with the presence of O_2. Combined with other noble metals or metal oxides, $Ce_{1-x}Bi_xO_{2-\delta}$ could activate the C-H bond in alcohol, leading the formation of active catalysts for HMF or other alcohol oxidation in alkaline aqueous solution.

Acknowledgements

The authors thank the National Natural Science Foundation of China. This work was supported by the National Natural Science Foundation of China (21273221).

Notes and references

[a] *State Key Laboratory of Rare Earth Resource Utilization, Changchun Institute of Applied Chemistry, Chinese Academy of Sciences, Changchun, Jilin 130022, China. E-mail: xgyang@ciac.ac.cn, yibozhang@ciac.ac.cn; Tel: 86-431-8526-2228*

[b] *University of Chinese Academy of Sciences, Beijing, 100039,China.*

[c] *Laboratory of Green Chemistry and Process, Changchun Institute of Applied Chemistry, Chinese Academy of Sciences, Changchun, Jilin 130022, China.*

[d] *The Northwest Research Institute of Chemistry Industry, Xi'an, Shaanxi, 710061, China.*

† Electronic Supplementary Information (ESI) available: Photograph, N_2 adsorption isotherms and pore size distributions of $Ce_{1-x}Bi_xO_{2-\delta}$ samples, SEM, ^1H NMR spectra, mass spectra, XRD, XPS and some control experiments. See DOI: 10.1039/b000000x/

1 T. Werpy and G. Petersen, *Top Value Added Chemicals from Biomass, Pacific Northwest National Laboratory*, 2004, **vol. 1**, 27.
2 Y. Roman-Leshkov, C. J. Barrett, Z. Y. Liu and J. A. Dumesic, *Nature*, 2007, **447**, 982-U985.
3 A. Corma, S. Iborra and A. Velty, *Chem. Rev.*, 2007, **107**, 2411-2502.
4 A. Osatiashtiani, A. F. Lee, D. R. Brown, J. A. Melero, G. Morales and K. Wilson, *Catal. Sci. Technol.*, 2014, **4**, 333-342.
5 D. A. Kotadia and S. S. Soni, *Catal. Sci. Technol.*, 2013, **3**, 469-474.
6 A. S. Amarasekara, D. Green and L. D. Williams, *Eur. Polym. J.*, 2009, **45**, 595-598.
7 A. Gandini, *Acs Symp. Ser.*, 1990, **433**, 195-208.
8 H. Hirai, *J. Macromol. Sci., Chem.*, 1984, **21**, 1165-1179.
9 C. Moreau, M. N. Belgacem and A. Gandini, *Top. Catal.*, 2004, **27**, 11-30.
10 P. Vinke, H. E. van Dam and H. van Bekkum, *New Dev. Select. Oxidat.*, 1990, **55**, 147-157.
11 P. Verdeguer, N. Merat and A. Gaset, *J. Mol. Catal.*, 1993, **85**, 327-344.
12 S. E. Davis, L. R. Houk, E. C. Tamargo, A. K. Datye and R. J. Davis, *Catal. Today*, 2011, **160**, 55-60.
13 S. Subbiah, S. P. Simeonov, J. Esperanca, L. P. N. Rebelo and C. A. M. Afonso, *Green Chem.*, 2013, **15**, 2849-2853.
14 B. Saha, S. Dutta and M. M. Abu-Omar, *Catal. Sci. Technol.*, 2012, **2**, 79-81.
15 O. Casanova, S. Iborra and A. Corma, *Chemsuschem*, 2009, **2**, 1138-1144.
16 N. K. Gupta, S. Nishimura, A. Takagaki and K. Ebitani, *Green Chem.*, 2011, **13**, 824-827.
17 S. E. Davis, B. N. Zope and R. J. Davis, *Green Chem.*, 2012, **14**, 143-147.
18 T. Pasini, M. Piccinini, M. Blosi, R. Bonelli, S. Albonetti, N. Dimitratos, J. A. Lopez-Sanchez, M. Sankar, Q. He, C. J. Kiely, G. J. Hutchings and F. Cavani, *Green Chem.*, 2011, **13**, 2091-2099.
19 Y. M. Shapiro, V. P. Smolyakov and V. G. Kulnevich, *Khimiya Geterotsiklicheskikh Soedinenii*, 1990, 741-744.
20 G. Hutchings, *Gold Bull.*, 2009, **42**, 260-266.
21 Y. Kuwauchi, H. Yoshida, T. Akita, M. Haruta and S. Takeda, *Angew. Chem., Int. Ed.*, 2012, **51**, 7729-7733.
22 W. Y. Song and E. J. M. Hensen, *Catal. Sci. Technol.*, 2013, **3**, 3020-3029.
23 M. Wang, F. Wang, J. Ma, M. Li, Z. Zhang, Y. Wang, X. Zhang and J. Xu, *Chem. Commun.*, 2014, **50**, 292-294.
24 N. Ta, J. Liu, S. Chenna, P. A. Crozier, Y. Li, A. Chen and W. Shen, *J. Am. Chem. Soc.*, 2012, **134**, 20585-20588.
25 A. Abad, P. Concepcion, A. Corma and H. Garcia, *Angew. Chem., Int. Ed.*, 2005, **44**, 4066-4069.
26 X. Liu, K. Zhou, L. Wang, B. Wang and Y. Li, *J. Am. Chem. Soc.*, 2009, **131**, 3140-3141.
27 N. Imanaka, T. Masui, K. Koyabu, K. Minami and T. Egawa, *Adv. Mater.*, 2007, **19**, 1608-1611.
28 D. Jiang, W. Wang, E. Gao, L. Zhang and S. Sun, *J. Phys. Chem. C*, 2013.
29 L. C. Glaeser, J. F. Brazdil, M. A. Hazle, M. Mehicic and R. K. Grasselli, *J. Chem. Soc., Faraday Trans.*, 1985, **81**, 2903-2912.
30 J. Zhu, D. Xiao, J. Li and X. Yang, *Cataly. Lett*, 2009, **129**, 240-246.
31 A. Karpenko, R. Leppelt, J. Cai, V. Plzak, A. Chuvilin, U. Kaiser and R. J. Behm, *J. Catal.*, 2007, **250**, 139-150.
32 L. Xue, C. Zhang, H. He and Y. Teraoka, *Catal. Today*, 2007, **126**, 449-455.
33 Z. Ma, H. Yin, S. Overbury and S. Dai, *Catal. Lett*, 2008, **126**, 20-30.
34 L. Li, F. Chen, J.-Q. Lu and M.-F. Luo, *J. Phys. Chem. A*, 2011, **115**, 7972-7977.
35 I. Kosacki, T. Suzuki, H. U. Anderson and P. Colomban, *Solid State Ionics*, 2002, **149**, 99-105.

36 M. Guo, J. Lu, Y. Wu, Y. Wang and M. Luo, *Langmuir*, 2011, **27**, 3872-3877.
37 L. Kumari, J. H. Lin and Y. R. Ma, *J. Phys.: Condens. Matter*, 2007, **19**.
38 V. N. Denisov, A. N. Ivlev, A. S. Lipin, B. N. Mavrin and V. G. Orlov, *J. Phys.: Condens. Matter*, 1997, **9**, 4967-4978.
39 S. Goswami, S. Dey and S. Jana, *Tetrahedron*, 2008, **64**, 6358-6363.
40 O. Casanova, S. Iborra and A. Corma, *J. Catal.*, 2009, **265**, 109-116.
41 J. Guzman, S. Carrettin, J. C. Fierro-Gonzalez, Y. L. Hao, B. C. Gates and A. Corma, *Angew. Chem., Int. Ed.*, 2005, **44**, 4778-4781.
42 J. Beckers, A. F. Lee and G. Rothenberg, *Adv. Synth. Catal.*, 2009, **351**, 1557-1566.
43 R. Sumathi, K. Johnson, B. Viswanathan and T. K. Varadarajan, *Appl. Catal., A*, 1998, **172**, 15-22.
44 M. Sankar, E. Nowicka, R. Tiruvalam, Q. He, S. H. Taylor, C. J. Kiely, D. Bethell, D. W. Knight and G. J. Hutchings, *Chem. – Eur. J.*, 2011, **17**, 6524-6532.
45 A. Abad, C. Almela, A. Corma and H. Garcia, *Tetrahedron*, 2006, **62**, 6666-6672.
46 B. T. Teng, J. J. Lang, X. D. Wen, C. Zhang, M. H. Fan and H. G. Harris, *J. Phys. Chem. C*, 2013, **117**, 18986-18993.
47 R. Si and M. Flytzani-Stephanopoulos, *Angew. Chem.*, 2008, **120**, 2926-2929.
48 J. Yang, Y. J. Guan, T. Verhoeven, R. van Santen, C. Li and E. J. M. Hensen, *Green Chem.*, 2009, **11**, 322-325.